Supplementary Information (SI) for Journal of Materials Chemistry A.

Supplementary Information

Mechanism of water vapor and SO_2 poisoning resistance in iron-fortified micron spherical $Ce_1Mn_7O_x$ for ultra-low temperature NH_3-SCR of NO_x

Xixi Chen$^{\Psi}$, Yongji Hu$^{\Psi}$, Yuesong Shen*.

State Key Laboratory of Materials-Oriented Chemical Engineering, Jiangsu Collaborative Innovation Center for Advanced Inorganic Function Composites, Jiangsu National Synergetic Innovation Center for Advanced Materials, College of Materials Science and Engineering, Nanjing Tech University, Nanjing 211816, China

* Corresponding author E-mail address: sys-njut@163.com

$^{\Psi}$ These authors contribute equally to this work

1. Sample Characterization

X-ray Diffraction (XRD)

The phase composition of the catalyst used to be characterized through Bruker D2 Phaser sequence X-ray powder diffractometer (XRD) geared up with a Cu/Kα X-ray supply (λ=0.154 nm). X-ray generator electricity was three kW. The scanning velocity was once 3°/min or 1°/min. 2θ scanning vary used to be 10-80°.

Field Emission Scanning Electron Microscopy (FE-SEM)

The microstructure of the synthesized catalyst particles used to be discovered through Tescan Mira four field emission scanning electron microscope (FE-SEM). The chosen sample powder used to be placed in the conductive adhesive and then sprayed gold. The field emission electron beam supply used to be used for irradiation imaging. The SEM imaging resolution was 1 nm and the acceleration voltage was once set to three kV.

High-Resolution Transmission Electron Microscopy (HR-TEM)

The high-magnification transmission electron microscope (HR-TEM, FEI Talos F200X G2) used to be used to gather TEM high-angle annular dark-field photographs and high-resolution photos to have a look at the interior morphological traits and crystal shape of the catalyst. The accelerating voltage was once 200 kV, the point resolution used to be 0.25 nm, and the line resolution used to be 0.12 nm.

N_2 adsorption and desorption

The specific surface area and pore volume distribution of the catalyst have been accrued by means of the surface area analyzer (Micromeritic TriStar 3000). The measurement of the sample powder was once managed beneath 100 meshes. The 0.1-0.2 g sample used to be vacuum degassed at 350 °C for 2 h and positioned in liquid nitrogen at -196 °C for determination. The specific surface area and pore volume distribution of the samples had been calculated based totally on BET and BJH equations.

Temperature programmed reduction of hydrogen (H_2-TPR)

The Semiautomatic Micromeritics AutoChem II 2920 instrument used to be used for the temperature programmed reduction of hydrogen (H_2-TPR). All the catalyst samples had been preheated to 400 °C beneath an argon move for 1 h and cooled to 50 °C. Then 5% H_2/Ar go with the flow was once switched, and the temperature multiplied from 50 °C to 800 °C at a 10 °C/min heating rate. The records had been accrued all through the total temperature range.

Temperature programmed desorption of NH_3 (NH_3-TPD)

The temperature programmed desorption of NH_3 (NH_3-TPD) was once decided with the aid of Micromeritics AutoChem II 2920 chemisorption analyzer. All the catalysts have been preheated at 400 °C beneath helium gasoline go with the flow for 1 h, and then cooled to 50 °C for ammonia adsorption. Afterward, ammonia used to be desorbed from 50 °C to 800 °C at a heating fee of 10 °C/min, and statistics had been accumulated over the whole temperature range.

X-ray Photoelectron Spectroscopy (XPS)

The valence states of distinctive elements in the catalyst had been analyzed by using Thermo Fsher K-Alpha X-ray photoelectron spectrometer. The instrument used 1361 eV monochromatic Al goal Kα ray as the radiation source, and the vacuum diploma used to be maintained at eight $\times 10^{-10}$ Pa. The sample used to be dried at 100 °C for 24 hours to get rid of moisture earlier than checking out and then examined besides any floor treatment. XPS spectra had been corrected with C 1s (284.8 eV) as the standard, and XPSPEAK 4.1 used to be used for top fitting.

in situ Diffuse Reflectance Infrared Fourier Transform Spectroscopy (DRIFTS)

The *in situ* adsorption of reactants and their intermediates on the catalyst floor was once detected the usage of a Bruker Vertex 80v vacuum FTIR spectrometer. Prior to catalyst testing, the samples have been required to be purged with a high-purity N_2 gasoline flow at 200 °C for 1 h to cast off the adsorbed impurities on the surface, and in consequence decreased to a preset temperature for every goal temperature historical past fee each 20 °C, observed via the passage of $NO+O_2+NH_3+N_2$ (1000 ppm NO, 1000 ppm NH_3, and 10% O_2) or/and H_2O/SO_2 (5 vol% H_2O and 50 ppm SO_2), every spectrum was achieved with 32 scans in the vary 800-4000 cm^{-1} with a resolution of 4 cm^{-1}. All spectra received have been routinely baseline corrected.

Density functional theory (DFT) calculations

Density functional theory (DFT) calculations had been carried out the usage of the Castep module (Clark et al., 2005) in the Material Studio 20.1 software, the use of the generalized gradient approximation (GGA) and the Revised-Perdew-Burke-Ernzerhof (RPBE) exchange-correlation functional. The Mn_3O_4-(112), Mn_3O_4-(103), Mn_3O_4-(211) and $MnFe_2O_4$-(311) facet buildings had been developed based totally on the XRD results, respectively, and all atoms have been satisfied till the energy change used to be much less than 1×10^{-5} eV/atom, the max displacement used to be much less than 0.001 Å, and the max stress per atom used to be much less than 0.03 eV/Å. The absorption energy was defined as [1]:

$$E_{ads} = E_{slab}^{A} - E_{slab} - E_{molecule},$$

where E_{ads} refers to the adsorption energy of the molecule, E_{slab}^{A} refers to the total energy of the system after the adsorption of the molecule on the adsorbent surface, E_{slab} refers to the energy of the adsorbent and $E_{molecule}$ refers to the energy of the molecule.

2. Computational Details

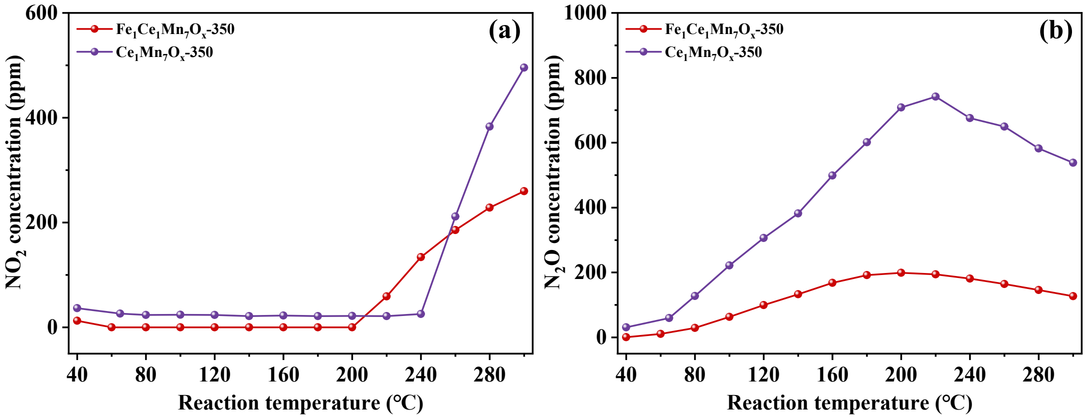

Figure S1. Concentrations of NO_2 and N_2O during N_2 selectivity test.

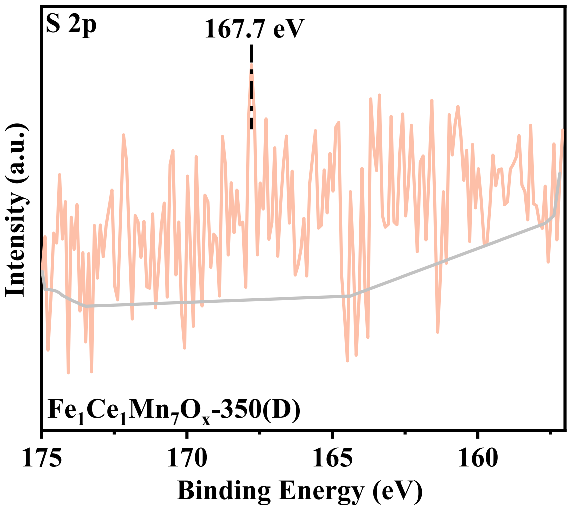

Figure S2. S2p XPS spectra of $Fe_1Ce_1Mn_7O_x$-350(D) catalyst.

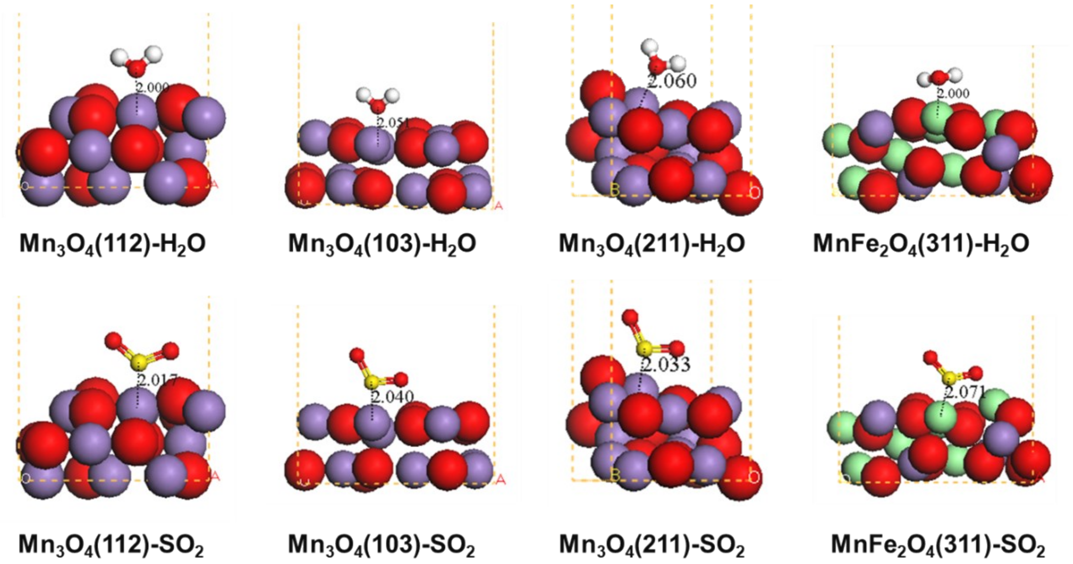

Figure S3. Structure of H_2O and SO_2 adsorption on the Mn_3O_4 (112), Mn_3O_4 (103), Mn_3O_4 (211) $MnFe_2O_4$ (311) surface before geometry optimization

Before optimization, the distance between H_2O molecules, SO_2 molecules and catalyst is all controlled at about 2Å to ensure that the calculation results can be compared.

3. Catalyst Performance Comparison

Supplementary Table 1 Summary of the performance of low-temperature catalysts in the absence/presence of SO_2 and H_2O

Catalyst	reaction condition[a]	NO conversion 1[b]	Poison condition[c]	NO conversion 2[d]	Ref
$CeMnO_x$	$[NO]=[NH_3]=500$ ppm, $[O_2]=3\%$, GHSV=60000 ml·g^{-1}·h^{-1}	>90% 125–275 °C	5% H_2O, 100 ppm SO_2	~70% (150 °C/8 h)	[2]
SM-E	$[NO]=[NH_3]=500$ ppm, $[O_2]=5\%$, GHSV=50000 h^{-1}	>90% 90–200 °C	5% H_2O, GHSV=150000 h^{-1}	>84% (130-350 °C)	[3]
FeCoMnCeSm/SiC	$[NO]=500$ppm, $[NH_3]=550$ ppm, $[O_2]=3\%$, GHSV=40000 h^{-1}	~100% 100–200 °C	5% H_2O, 100 ppm SO_2	70% (200 °C/13 h)	[4]
Ce-Ti/MnO_2	$[NO]=[NH_3]=600$ ppm, $[O_2]=5\%$, GHSV=40000 h^{-1}	~100% 100–200 °C	10% H_2O, 50 ppm SO_2	85.2% (150 °C/12h)	[5]
CM/CSZ-IM	$[NO]=[NH_3]=350$ ppm, $[O_2]=15\%$, GHSV=400 L·g·h^{-1}	>90% 200–320 °C	/	/	[6]
$Cu_{2.5}$-SSZ-39-Z	$[NO]=[NH_3]=500$ ppm, $[O_2]=5\%$, GHSV=200000 h^{-1}	>90% 225–550 °C	/	/	[7]
$Cu_{0.2}$Ce/CAC-CNT	$[NO]=[NH_3]=500$ ppm, $[O_2]=5\%$, GHSV=10000 h^{-1}	~100% 150–200 °C	5% H_2O, 50 ppm	91.2% (150 °C/8h)	[8]
Mn-BTC-335 °C	$[NO]=[NH_3]=500$ ppm, $[O_2]=5\%$, GHSV=108000 h^{-1}	>70% 180–330 °C	6% H_2O, 100 ppm	43% (150 °C/8h)	[9]
Fe-$Ce_1Mn_7O_x$-350	$[NO]=[NH_3]=1000$ ppm, $[O_2]=10\%$, GHSV=20000 h^{-1}	>91% 54-275 °C	5% H_2O, 50 ppm	~99%(127 °C/30h)	This work
$Ce_1Mn_7O_x$-350	$[NO]=[NH_3]=1000$ ppm, $[O_2]=10\%$, GHSV=20000 h^{-1}	>91% 59-255 °C	5% H_2O, 50 ppm	~88% (150 °C/8h)	This work

a Reaction gas mixture and GHSV.

b NO conversion at a specified temperature.

c The concentration of SO_2 and H_2O introduced on the basis of reaction gas.

d NO conversion at a certain temperature after introducing SO_2 and/or H_2O for a specified time

Supplementary Table 2 Element percentage of $Fe_1Ce_1Mn_7O_x$-350, $Fe_1Ce_1Mn_7O_x$-350(D) and $Ce_1Mn_7O_x$-350 catalyst determined by XPS.

catalyst	Ce	Mn	Fe	O	S
$Ce_1Mn_7O_x$-350	6.78%	24.11%	\	69.11%	\
$Fe_1Ce_1Mn_7O_x$-350	4.72%	24.15%	5.59%	65.53%	\
$Fe_1Ce_1Mn_7O_x$-350(D)	5.54%	22.24%	6.07%	65.47%	0.67%

Supplementary Table 3 The unit cell parameters used in DFT calculations.

Crystal phase	Space group	a(Å)	c(Å)
Mn_3O_4	I41/amd	5.83	9.55
$MnFe_2O_4$	Fd-3m	8.52	\

Reference

[1] T. Cheng, J. Li, X. Ma, L. Zhou, H. Wu, L. Yang, Alkylation modified pistachio shell-based biochar to promote the adsorption of VOCs in high humidity environment star, Environ. Pollut., 295 (2022) 118714.

[2] S. Shi, S. Li, Y. Yang, C. Deng, C. Xu, J. Yang, D. Zhao, S. Wang, S. Ding, C. Chen, Mechanochemically engineered Brønsted acidity on metal oxides for enhanced low-temperature NO_x removal, Sep. Purif. Technol., 364 (2025) 132497.

[3] F. Wang, P. Wang, T. Lan, Y. Shen, W. Ren, D. Zhang, Ultralow-Temperature NO_x Reduction over $SmMn_2O_5$ Mullite Catalysts Via Modulating the Superficial Dual-Functional Active Sites, ACS Catal, (2022).

[4] H. Duan, F. Zhang, M. Zhang, T. Ma, Z. Xin, Q. Gao, J. Zai, SiC-Supported Polymetallic Oxide Catalysts for Enhanced Low-Temperature SCR Denitration, ENERG FUEL, 39 (2025) 6400-6411.

[5] S. Jingjing, L. Shaomian, J. Yongjun, X. Wenqing, Y. Jian, L. Bing, C. Wenxing, Z. Jianling, J. Lihua, Z. Tingyu, Z. Ziyi, X. Guangwen, S. Fabing, Dual single-atom Ce-Ti/MnO_2 catalyst enhances low-temperature NH_3-SCR performance with high H_2O and SO_2 resistance, NANO RES, (2022).

[6] T. Andana, K.G. Rappé, N.C. Nelson, F. Gao, Y. Wang, Selective catalytic reduction of NOx with NH_3 over Ce-Mn oxide and Cu-SSZ-13 composite catalysts – Low temperature enhancement, APPL CATAL B-ENVIRON, (2022).

[7] D. Jinpeng, H. Shichao, H. Chi, S. Yulong, Z. Yan, S. Wenpo, H. Hong, Comparison of precursors for the synthesis of Cu-SSZ-39 zeolite catalysts for NH_3-SCR reaction, APPL CATAL B-ENVIRON, (2023).

[8] L. Yang, P. Wang, L. Yao, X. Meng, C.Q. Jia, X. Jiang, W. Jiang, Copper Doping Promotion on Ce/CAC-CNT Catalysts with High Sulfur Dioxide Tolerance for Low-Temperature NH_3–SCR, ACS SUSTAIN CHEM ENG, (2021).

[9] S. Kunli, G. Kaiyu, M. Siman, M. Dandan, L. Yixuan, H. Chi, W. Hongkang, C. Yonghong, S. Jian-Wen, Insight into the Origin of Excellent SO_2 Tolerance and de-NO_x Performance of quasi-Mn-BTC in the Low-Temperature Catalytic Reduction of Nitrogen Oxide, ACS Catal, (2023).